JACS
JOURNAL OF THE AMERICAN CHEMICAL SOCIETY

Communication

pubs.acs.org/JACS

Dissolution and Liquid Crystals Phase of 2D Polymeric Carbon Nitride

Zhixin Zhou, Jianhai Wang, Jiachao Yu, Yanfei Shen, Ying Li, Anran Liu, Songqin Liu, and Yuanjian Zhang*

Jiangsu Province Hi-Tech Key Laboratory for Bio-Medical Research, Jiangsu Optoelectronic Functional Materials and Engineering Laboratory, School of Chemistry and Chemical Engineering, Medical School, Southeast University, Nanjing 211189, China

Supporting Information

ABSTRACT: Graphite-phase polymeric carbon nitride (GPPCN) has emerged as a promising metal-free material toward optoelectronics and (photo)catalysis. However, the insolubility of GPPCN remains one of the biggest impediments toward its potential applications. Herein, we report that GPPCN could be dissolved in concentrated sulfuric acid, the first feasible solvent so far, due to the synergistic protonation and intercalation. The concentration was up to 300 mg/mL, thousands of time higher than previous reported dispersions. As a result, the first successful liquid-state NMR spectra of GPPCN were obtained, which provides a more feasible method to reveal the finer structure of GPPCN. Moreover, at high concentration, a liquid crystal phase for the carbon nitride family was first observed. The successful dissolution of GPPCN and the formation of highly anisotropic mesophases would greatly pave the potential applications such as GPPCN-based nanocomposites or assembly of marcroscopic, ordered materials.

Regarded as one kind of nitrogen-doped carbon materials, carbon nitrides have been received tremendous attention because of delocalized conduction and valence bands, which are conducive to charge transport and tunable band gap ranging up to 5 eV.[1] Among them, graphite-phase polymeric carbon nitride (C/N/H, denoted as GPPCN), synthesized by thermal condensation of urea, dicyandiamide, melamine, and other *s*-triazine heterocyclic compounds (see molecular structure in Figure S1), is known as a new generation of metal-free polymeric semiconductor for environment remediation, such as photocatalytic H_2 evolution from water,[2] photodegradation of organic pollutants,[3] photoelectric conversion,[4] CO_2 activation,[5] and other important catalytic reactions.[6]

However, as was the case in the early days of graphene and carbon nanotubes (CNTs) research,[7] the insolubility/difficult dispersion of GPPCN in any solvents remains one of the biggest impediments to the realization of their potential applications. For instance, liquid crystal and fluid-phase assembly for macroscopic, ordered structures which need sufficient solubility or dispersibility,[8] have not been reported so far. Moreover, insolubility makes some basic characterizations difficult, resulting in lack of thorough insights into the optical properties like the absorption coefficient ε concerning the nature of GPPCN[9] and a long-term controversial discussion regarding finer details of their local structures.[10] Recently, several pioneering works revealed that bulk GPPCN could be exfoliated into 2D single/few layer sheets and dispersed in water or other organic solvents by sonication.[11] Nevertheless, the limitation of these liquid-phase dispersions includes: (1) it often needs over 10 h of sonication but yields low concentrations (0.15 mg/mL, ref 11a), and (2) sonication limits the size of GPPCN achievable and changes the electronic structure of GPPCN.

Herein, we report that GPPCN could be dissolved and form true thermodynamic solutions in concentrated sulfuric acid which is widely used in addressing the insolubility of graphitic materials[8a,c] and processing Kevlar fiber in industry.[12] The concentration of GPPCN solution could be up to 300 mg/mL (~14 wt %) at room temperature, 2000 times higher than those of previous dispersion.[11a] As a result, the first successful liquid-state NMR spectra of GPPCN were obtained, which displays much higher resolution compared with solid-state one, thus offering more feasible characterization toward more reliable structural information on GPPCN. More interestingly, due to the sufficient dissolution, the lyotropic liquid crystal phase of GPPCN was also observed at high concentration. Our solubilization method would open a new vista to process GPPCN for much broader applications such as in the form of nanocomposites and fluid-phase assembly for macroscopic-ordered structures.

The dissolution behavior of GPPCN in concentrated sulfuric acid was first investigated. Figure 1a shows bulk GPPCN turned into a clear pale yellow solution after being stirred with concentrated sulfuric acid at 100 °C for 2 h. Moreover, the concentration of GPPCN/H_2SO_4 solution could be prepared up to 300 mg/mL (~14 wt %) at room temperature. Like most other compounds, higher temperature is favored for dissolution

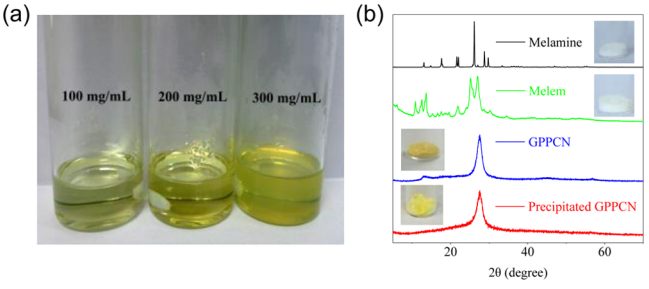

Figure 1. (a) Photo of bulk GPPCN dissolved in concentrated sulfuric acid at different concentrations. (b) XRD patterns of melamine, melem, GPPCN, and the GPPCN precipitated from GPPCN/H_2SO_4 solution using methanol. Inset: photos of respective powders.

Received: November 28, 2014
Published: January 29, 2015

DOI: 10.1021/ja512179x
J. Am. Chem. Soc. 2015, 137, 2179–2182

(Figure S2), and the Tyndall effect was normally not observed for GPPCN/H_2SO_4 solution (Figure S3), indicating the formation of a true solution instead of a colloidal system. GPPCN solution was stable without aggregating upon standing for more than one year. Fuming sulfuric acid (30.0−33.0% SO_3) without any water was also capable of dissolving GPPCN with a similar behavior. For experimental convenience, concentrated sulfuric acid was used as the solvent for GPPCN in the following studies.

As known, concentrated sulfuric acid is corrosive on many materials, mainly ascribing to its strong dehydrating and oxidizing properties. Thus, we may concern whether GPPCN was decomposed in concentrated sulfuric acid or not. Indeed, since few oxygen atoms exist in GPPCN, the dehydrating may not occur. GPPCN should also be rather stable against oxidation if considering the fact that GPPCN is prepared by condensation in a strong oxidation environment (550 °C in air) and its highest occupied molecular orbital (HOMO) posits at 1.83 V vs NHE,[4b] close to the standard electrode potential of noble metal (e.g., Au^+/Au).[13] This assumption was further supported by the following experiments. First, the GPPCN/H_2SO_4 solution was found to have the same maximum PL emission peak at 465 nm (Figure S4) as the original bulk GPPCN, indicating the preservation of the electronic structure from bulk GPPCN, i.e., the conjugated −C−N− network, was mostly retained after dissolution. Second, GPPCN could be extracted from GPPCN/H_2SO_4 solution using poor solvents such as methanol. Evidently, the X-ray diffraction (XRD) shows the precipitated GPPCN had the identical predominant 002 diffraction as the pristine bulk GPPCN (Figure 1b), which offered a direct evidence for the conservation of stacked 2D GPPCN networks after dissolution and precipitation. The slight increase of the peak width would be owing to formation of expanded or turbostratic GPPCN.[14] In contrast, the XRD patterns of the small subunits for GPPCN such as melamine and melem (Figure 2b) are quite different to that of pristine GPPCN. Moreover, the color of the precipitated GPPCN was still yellow by naked eyes, but the small subunits for GPPCN, such as melamine and melem, are white (Figure 2b inset), indicating GPPCN dissolved in H_2SO_4 was not disintegrated into small subunits. The slight color change of precipitated GPPCN was noted, which was due to the protonation of GPPCN with H_2SO_4 (Figure S5).[4a]

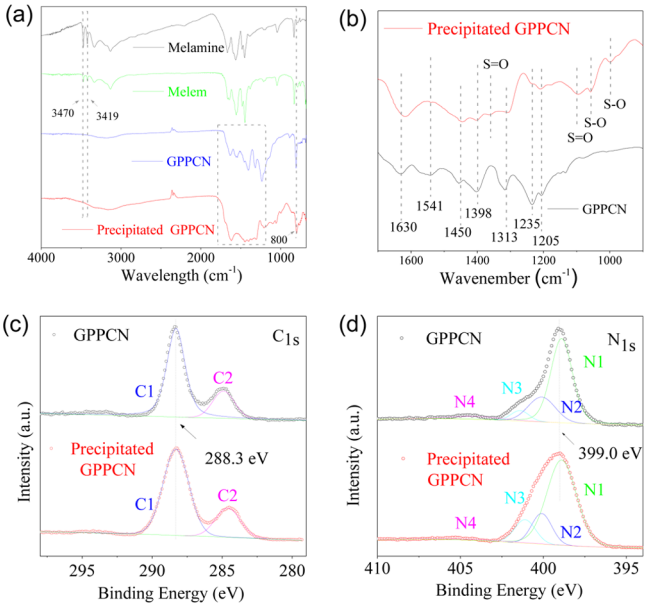

Figure 2. FT-IR (a) spectra of melamine, melem, GPPCN, and the GPPCN precipitated from GPPCN/H_2SO_4 solution using methanol. Enlarged FT-IR spectra of GPPCN and precipitated GPPCN from 1700 to 900 cm^{-1} showing more details (b). XPS C_{1s} (c) and N_{1s} (d) spectra of pristine GPPCN and the precipitated GPPCN.

To further probe the chemical structure of the precipitated GPPCN, the FT-IR and X-ray photoelectron spectroscopy (XPS) analysis were performed. The characteristic FT-IR spectrum of the precipitated GPPCN (Figure 2a) is largely reminiscent of that of the bulk GPPCN, both having peaks at 800 cm^{-1} (tri-*s*-triazine ring out of plane bending), 3000−3500 cm^{-1} (NH stretching) and 1200−1700 cm^{-1}.[11b] The vibrations at 1630 (C═N), 1541 (C═N), 1450 (C−N), 1398 (C−N), 1313 (C−N), 1235 (C−N), and 1205 cm^{-1} (C−N) were retained for the precipitated GPPCN, but the intensity of them was slightly changed with respect to those of GPPCN. The changes may result from the protonation of GPPCN with H_2SO_4.[4a,15] Moreover, characteristic peaks at 3470 and 3419 cm^{-1} of $\nu(-NH_2)$ were not observed for the precipitated GPPCN, while observed for the subunits for GPPCN such as melamine and melem, further ruling out the decomposition of GPPCN into small subunits during the dissolution. In addition, the vibration peaks of S−O and S═O in SO_4^{2-} was also observed (Figure 2b), in agreement with S_{2p} and O_{1s} XPS spectra (Figure S6), which was due to the protonation of GPPCN with H_2SO_4. The C_{1s} XPS spectra in Figure 2c show one predominant C1 peak with a binding energy (BE) of ∼288.3 eV for both pristine GPPCN and the precipitated GPPCN, corresponding to the typical aromatic C−N═C coordination in a GPPCN framework.[1a] The C2 peak with BE of 284.6 eV was ascribed to carbon impurities.[1a,11a] Meanwhile, four N_{1s} peaks (N1−N4) assigning to −C═N−C, $N-(C)_3$, C−NH and charged effect respectively, were observed for both pristine and precipitated GPPCN.[1a] The relative intensity of N3 of the precipitated GPPCN increased slightly due to the occurrence of the protonation. Further XPS quantitative analysis (Table S1) shows the precipitated GPPCN exhibits a C/N ratio of 0.73, close to the ideal fully condensed C_3N_4 (C/N = 0.75) and the same to that of bulk GPPCN sample (C/N = 0.73), indicating that the chemical composition of carbon and nitrogen in polymeric carbon nitride was retained during the dissolution and precipitation process. In contrast, the subunits of GPPCN such as melon (0.67), melem (0.6), melamine (0.5), and urea (0.5) have a much lower C/N ratio (see molecular structures in Figure S1).

Therefore, combing results of PL, XRD, XPS, and FT-IR analysis, the typical stacked lamellar texture, electronic structure, chemical composition, and tri-*s*-triazine related bonding of GPPCN was well maintained after dissolution in concentrated sulfuric acid, suggesting GPPCN was mostly dissolved in concentrated sulfuric acid rather than significantly decomposed. The minor molecular changes of the precipitated GPPCN came from the protonation by H_2SO_4,[4a,15] which offered a stronger interaction than the general solvolytic interaction. Indeed, nitrogen-rich engineering plastics[16] and other graphite-like materials are similarly processed in concentrated sulfuric acid without any decomposition.[8a,c,14,17]

To get insight of the dissolution process, the mechanism of GPPCN dissolution in sulfuric acid was further investigated. Earlier work demonstrated that the protonation of SWNTs sidewalls, resulting in electrostatic repulsion, played an important role in dispersing SWNTs in concentrated H_2SO_4.[8a,c] As shown in FT-IR and XPS spectra (Figures 2 and S6), GPPCN was

DOI: 10.1021/ja512179x
J. Am. Chem. Soc. 2015, 137, 2179−2182

protonated during the dissolution. In order to better understand the role of H_2SO_4 in dissolving GPPCN, the GPPCN/H_2SO_4 paste (600 mg/mL, Figure S7), the intermediate states during the solvation, was prepared (see Experimental in Supporting Information). It was reported that lone pair electron of the "aromatic" nitrogen atoms were prone to interacting with proton, leading to the blue-shift absorption.[4] Thus, the degree of blue-shift absorption could be used to evaluate the degrees of protonation. Figure 3a shows the typical UV−vis absorption edge

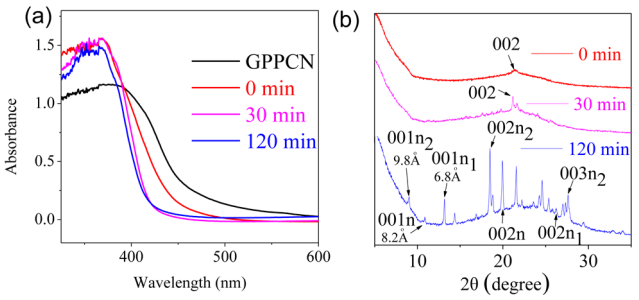

Figure 3. (a) UV−vis absorption of GPPCN and the intermediate states of GPPCN/H_2SO_4 during the solvation in H_2SO_4 from 0, 30, to 120 min. (b) The corresponding XRD patterns of the intermediate states; n_1 and n_2 indicate reflections of the stage-1 and -2 intercalation, and n indicates reflections of the intercalation with H_2SO_4.

of GPPCN was mostly maintained but gradually blue-shifted from 465 to 380 nm, mirroring that the degree of protonation gradually increased with the increase of heating time during the dissolution in H_2SO_4.

For comparison, other common mineral acids such as HNO_3 and HCl were also investigated to dissolve GPPCN, but the solubility was negligible (Figure S5), indicating the protonation was not the only successful factor for dissolving GPPCN. In the family of lamellar materials, intercalation reactions are often used as the one of most important steps in exfoliation of lamellar crystals to individual atomic/molecular layers. Due to the structural similarity, it was supposed that the intercalation reaction might also occur for GPPCN. After formation of GPPCN/H_2SO_4 paste without heating, Figure 3b (red curve) shows that the 002 peak in its XRD pattern was broadened and shifted toward smaller angle compared with that of pristine GPPCN (Figure 1b, blue curve). This could be attributed to the formation of expanded GPPCN (the corresponding interlayer distance increased from 0.33 to 0.37 nm), the beginning of delamination. Heating is typically used to accelerate the intercalation rate. It was found that the 002 peak became noticeable and was shifted toward smaller 2θ values after heating at 100 °C for 30 min. When heating at 100 °C for 120 min, the new diffraction line appeared at 13.1°, which could be ascribed to 001 peak of stage-1 intercalation (see scheme in Figure S8) The corresponding interlayer distance was 0.68 nm, which was sufficient to accommodate a single layer of intercalated acid molecules. This was consistent with the d_{001} distance in stage-1 h-BN intercalation compounds with sulfuric acid (0.69 nm).[17] In addition to the stage-1 intercalation, the 001 characteristic reflection of stage-2 was observed with an interlayer distance 0.98 nm. The difference of interlayer distance between stages-1 and -2 was 0.3 nm (0.98 nm -0.68 nm), similar to that of intercalated graphite with H_2SO_4 (0.31 nm).[18] Another new phase with d_{001} = 0.82 nm that might indicate the formation of hydrated sulfate species inside the GPPCN matrix was also observed, reminiscent of the intercalation reaction of h-BN with H_2SO_4.[17] Notably, the corresponding 00l was also observed, which was in good agreement with the 001 peak. Several new reflections, which were ruled out as the decomposed product due to the distinct difference between them in XRD pattern (Figure S9), may be caused by formation of some higher stage intercalation phases (see scheme in Figure S8), indicating a mixed-stage intercalation for GPPCN with sulfuric acid.[14,17,19]

More evidently, GPPCN could be precipitated from GPPCN solution with the same interlayer distance of original GPPCN (Figure 1b), manifesting the intercalation was reversible and implying that no irreversible covalent bonds form to the GPPCN layers during the dissolution process. Therefore, through protonation and intercalation reaction that would ensure sufficient electrostatic repulsion and debundling among GPPCN sheets, GPPCN could be dissolved in H_2SO_4. Nevertheless, it should be noted that although the intercalation of lamellar materials by strong acids has been studied for decades,[8a,19] there are few reports of dissolving lamellar materials in strong acids. The unusual dissolution behavior of GPPCN here might be due to its unique organic properties.[16]

One of the foreseeable benefits of dissolving GPPCN was that some structural characterizations, but limited by solid-state sampling before, became applicable. For example, the molar extinction coefficient (ε) was thus capable of being measured to evaluate the probability of the electronic transition and the concentration of g-CN, which was vital for guiding their applications such as photocatalysis and photoelectrochemistry. Here, the UV−vis absorption spectra of g-CN solution with different concentration (Figure S10) can be measured, showing Lambert−Beer behavior for all diluted solutions and ε of 1147.6 L g^{-1} m^{-1} at 295 nm that was similar to graphene materials.[8a] As another example, the liquid-state ^{15}N (Figure 4a) and ^{13}C (Figure

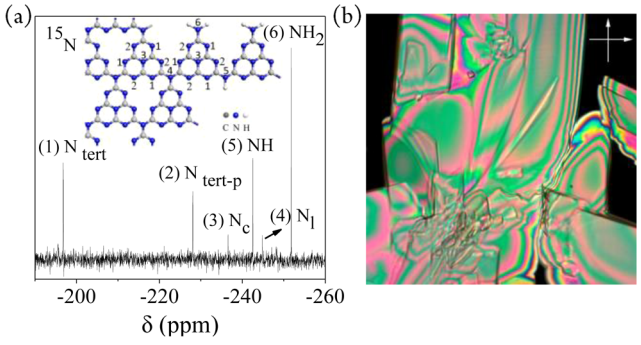

Figure 4. (a) ^{15}N liquid-state NMR spectrum of GPPCN/H_2SO_4 solution; inset: the proposed structure for GPPCN. (b) Optical textures of GPPCN/H_2SO_4 under a polarizing microscope (crossed polarizer, magnification ×20).

S11) NMR spectra of GPPCN in concentrated sulfuric acid-d_2 were successfully recorded with much higher resolution compared with the solid-state one. As outlined in the ^{15}N NMR spectrum of GPPCN (Figure 4a), clear-cut signals without any overlapping were observed. The full width at half height (fwhh, 0.04−0.07 ppm) was hundreds times narrower than the solid-state one (3−18 ppm) in previous reports.[10b] Hence, it provided a much easier way to disclose the structure of GPPCN in principle, for instance, here the peaks could be assigned to six different N in GPPCN (Figure 4a inset, see more discussion in Supporting Information). Undoubtedly, the successful dissolution of GPPCN would offer more feasible characterizations

DOI: 10.1021/ja512179x
J. Am. Chem. Soc. 2015, 137, 2179−2182

toward more reliable structural information. Nevertheless, it should be noted that giving a full identification for the structure of GPPCN is out of the scope of this work. Due to the structural complexity of GPPCN, more investigations are still needed.

As known, several crystalline phases of carbon nitrides have been predicted (e.g., super hard β-C_3N_4)[20] and synthesized (e.g., graphitic-C_3N_4[21] and GPPCN). However, to the best of our knowledge, liquid-crystalline phases of the carbon nitride family have never been reported so far due to the lack of a sufficient solubility in any solvents in previous studies, but it is of great interest due to their significance in producing large, oriented materials from nanoscale building blocks by fluid-phase assembly.[8] The formation of liquid-crystalline phases of polymeric carbon nitride at high concentration was verified by examining birefringence in an optical microscope with crossed polarizers. It was found that the solution of GPPCN/H_2SO_4 (600 mg/mL) above 150 °C was isotropic. When the temperature decreased to ∼60 °C, the liquid crystal phase was observed, and its anisotropic refractive index altered the polarization of transmitted light, resulting in light and dark patterns on the micron scale. Figure 4b shows birefringence typical of a liquid crystal under a cross-polarizer, and the liquid-crystalline Schlieren texture of GPPCN/H_2SO_4 was very similar to typical nematic samples.[8a,22] The adequate movements and self-assembling of 2D carbon nitride layer in H_2SO_4 that benefited from the sufficient dissolution and the high rigidity of carbon nitride framework were supposed to play important roles in the formation of liquid crystal phase.

In summary, we showed that bulk graphite-phase polymeric carbon nitride (C/N/H, denoted as GPPCN) could be dissolved in concentrated sulfuric acids up to 300 mg/mL (∼14 wt %) at room temperature. It was found that the acid protonated the GPPCN to induce electrostatic repulsion and the intercalation made GPPCN interlayer separate, two important synergistic factors for the successful dissolution. As a result, the characterizations limited by solid-state sampling before, such as the molar extinction coefficient and high resolution liquid-state NMR spectra of GPPCN, were first measured, and the liquid crystal phase of GPPCN was first observed. Our solubilization strategy provided a new way to better understand fundamental physicochemical properties of as-prepared bulk GPPCN. Similar to the research of graphene and CNTs dissolved in concentrated sulfuric acids, the highly concentrated isotropic and liquid-crystalline phase are promising for functionalization and for scalable manufacturing of nanocomposites and films.[8a,c]

■ ASSOCIATED CONTENT

Supporting Information

Experiment details, Figures S1−S11, Tables S1 and S2, and more discussions. This material is available free of charge via the Internet at http://pubs.acs.org.

■ AUTHOR INFORMATION

Corresponding Author

*Yuanjian.Zhang@seu.edu.cn

Notes

The authors declare no competing financial interest.

■ ACKNOWLEDGMENTS

This work was supported in part by the National Natural Science Foundation of China (21203023, 91333110, 21305065) and NSF of Jiangsu province (BK2012317, BK20130788) for financial support. We thank Prof. Hong Yang (SEU) for liquid crystal characterization and helpful discussion.

■ REFERENCES

(1) (a) Lin, Z. Z.; Wang, X. C. *Angew. Chem., Int. Ed.* **2013**, *52*, 1735. (b) Deifallah, M.; McMillan, P. F.; Cora, F. *J. Phys. Chem. C* **2008**, *112*, 5447. (c) Vinu, A.; Ariga, K.; Mori, T.; Nakanishi, T.; Hishita, S.; Golberg, D.; Bando, Y. *Adv. Mater.* **2005**, *17*, 1648.

(2) (a) Wang, X. C.; Maeda, K.; Thomas, A.; Takanabe, K.; Xin, G.; Carlsson, J. M.; Domen, K.; Antonietti, M. *Nat. Mater.* **2009**, *8*, 76. (b) Xiang, Q. J.; Yu, J. G.; Jaroniec, M. *J. Phys. Chem. C* **2011**, *115*, 7355.

(3) Yan, S. C.; Li, Z. S.; Zou, Z. G. *Langmuir* **2009**, *25*, 10397.

(4) (a) Zhang, Y.; Thomas, A.; Antonietti, M.; Wang, X. *J. Am. Chem. Soc.* **2009**, *131*, 50. (b) Zhang, Y. J.; Antonietti, M. *Chem.—Asian J.* **2010**, *5*, 1307.

(5) Goettmann, F.; Thomas, A.; Antonietti, M. *Angew. Chem., Int. Ed.* **2007**, *46*, 2717.

(6) (a) Zheng, Y.; Jiao, Y.; Chen, J.; Liu, J.; Liang, J.; Du, A.; Zhang, W. M.; Zhu, Z. H.; Smith, S. C.; Jaroniec, M.; Lu, G. Q.; Qiao, S. Z. *J. Am. Chem. Soc.* **2011**, *133*, 20116. (b) Zhang, P. F.; Gong, Y. T.; Li, H. R.; Chen, Z. R.; Wang, Y. *Nat. Commun.* **2013**, *4*, 1593. (c) Li, X. H.; Chen, J. S.; Wang, X. C.; Sun, J. H.; Antonietti, M. *J. Am. Chem. Soc.* **2011**, *133*, 8074.

(7) Tasis, D.; Tagmatarchis, N.; Bianco, A.; Prato, M. *Chem. Rev.* **2006**, *106*, 1105.

(8) (a) Behabtu, N.; Lomeda, J. R.; Green, M. J.; Higginbotham, A. L.; Sinitskii, A.; Kosynkin, D. V.; Tsentalovich, D.; Parra-Vasquez, A. N. G.; Schmidt, J.; Kesselman, E.; Cohen, Y.; Talmon, Y.; Tour, J. M.; Pasquali, M. *Nat. Nanotechnol.* **2010**, *5*, 406. (b) Xu, Z.; Gao, C. *Nat. Commun.* **2011**, *2*, 571. (c) Davis, V. A.; Parra-Vasquez, A. N. G.; Green, M. J.; Rai, P. K.; Behabtu, N.; Prieto, V.; Booker, R. D.; Schmidt, J.; Kesselman, E.; Zhou, W.; Fan, H.; Adams, W. W.; Hauge, R. H.; Fischer, J. E.; Cohen, Y.; Talmon, Y.; Smalley, R. E.; Pasquali, M. *Nat. Nanotechnol.* **2009**, *4*, 830.

(9) Merschjann, C.; Tyborski, T.; Orthmann, S.; Yang, F.; Schwarzburg, K.; Lublow, M.; Lux-Steiner, M. C.; Schedel-Niedrig, T. *Phys. Rev. B* 2013, *87*.

(10) (a) Kroke, E.; Schwarz, M.; Horath-Bordon, E.; Kroll, P.; Noll, B.; Norman, A. D. *New J. Chem.* **2002**, *26*, 508. (b) Lotsch, B. V.; Doblinger, M.; Sehnert, J.; Seyfarth, L.; Senker, J.; Oeckler, O.; Schnick, W. *Chem.—Eur. J.* **2007**, *13*, 4969.

(11) (a) Zhang, X.; Xie, X.; Wang, H.; Zhang, J.; Pan, B.; Xie, Y. *J. Am. Chem. Soc.* **2013**, *135*, 18. (b) Yang, S.; Gong, Y.; Zhang, J.; Zhan, L.; Ma, L.; Fang, Z.; Vajtai, R.; Wang, X.; Ajayan, P. M. *Adv. Mater.* **2013**, *25*, 2452. (c) Xu, J.; Zhang, L. W.; Shi, R.; Zhu, Y. F. *J. Mater. Chem. A* **2013**, *1*, 14766.

(12) Yang, H. H. *Aromatic High-Strength Fibers*; Wiley: New York, 1989.

(13) Bard, A. J.; Faulker, R. L. *Electrochemical Methods Fundamentals and Applications*; 2nd ed.; Wiley: New York, 2001.

(14) Dimiev, A. M.; Bachilo, S. M.; Saito, R.; Tour, J. M. *ACS Nano* **2012**, *6*, 7842.

(15) (a) Jurgens, B.; Irran, E.; Senker, J.; Kroll, P.; Muller, H.; Schnick, W. *J. Am. Chem. Soc.* **2003**, *125*, 10288. (b) Sattler, A.; Seyfarth, L.; Senker, J.; Schnick, W. *Z. Anorg. Allg. Chem.* **2005**, *631*, 2545.

(16) Inoue, S.; Imai, Y.; Uno, K.; Iwakura, Y. *Makromol. Chem.* **1966**, *95*, 236.

(17) Kovtyukhova, N. I.; Wang, Y. X.; Lv, R. T.; Terrones, M.; Crespi, V. H.; Mallouk, T. E. *J. Am. Chem. Soc.* **2013**, *135*, 8372.

(18) Dimiev, A. M.; Ceriotti, G.; Behabtu, N.; Zakhidov, D.; Pasquali, M.; Saito, R.; Tour, J. M. *ACS Nano* **2013**, *7*, 2773.

(19) Dresselhaus, M. S.; Dresselhaus, G. *Adv. Phys.* **2002**, *51*, 1.

(20) Liu, A. Y.; Cohen, M. L. *Science* **1989**, *245*, 841.

(21) Algara-Siller, G.; Severin, N.; Chong, S. Y.; Bjorkman, T.; Palgrave, R. G.; Laybourn, A.; Antonietti, M.; Khimyak, Y. Z.; Krasheninnikov, A. V.; Rabe, J. P.; Kaiser, U.; Cooper, A. I.; Thomas, A.; Bojdys, M. J. *Angew. Chem., Int. Ed.* **2014**, *53*, 7450.

(22) Chandrasekhar, S. *Liquid Crystals*; 2nd ed.; Cambridge University Press: New York, 1992.

DOI: 10.1021/ja512179x
J. Am. Chem. Soc. 2015, 137, 2179−2182